

Effect and mechanism of asiatic acid on autophagy in myocardial ischemia-reperfusion injury *in vivo* and *in vitro*

CHENLONG YI^{1*}, LINJIE SI^{2*}, JING XU², JUNYI YANG³, QIANG WANG¹ and XIAOWEI WANG²

¹Department of Cardiovascular Surgery, Northern Jiangsu People's Hospital, Clinical Medical College, Yangzhou University, Yangzhou, Jiangsu 225001; ²Department of Thoracic and Cardiovascular Surgery, The First Affiliated Hospital of Nanjing Medical University; ³Department of Thoracic and Cardiovascular Surgery, Jiangsu Province Hospital of Traditional Chinese Medicine (TCM), Nanjing, Jiangsu 210029, P.R. China

Received August 6, 2019; Accepted May 20, 2020

DOI: 10.3892/etm.2020.9182

Abstract. Myocardial ischemia-reperfusion injury (MIRI) is a major cause of heart failure in patients with coronary heart disease. The excessive accumulation of reactive oxygen species (ROS) during MIRI induces the overactivation of an autophagic response, which aggravates myocardial cell damage. Asiatic acid (AA) is a triterpenoid compound, which is extracted from *Centella asiatica* and exhibits a variety of pharmacological effects such as hepatoprotective, neuroprotective and antioxidant. However, the association of AA with autophagy in MIRI is not fully understood. In the present study, the positive effects of AA in MIRI injury were determined via establishing a MIRI mouse model. Pre-treatment with AA was indicated to improve cardiac function and decrease cardiomyocyte autophagy in mice subjected to MIRI. To examine the protective effects of AA and the underlying mechanisms in MIRI, a cardiomyocyte glucose deprivation/reperfusion (OGD) model was established. The administration of AA decreased the levels of ROS and malondialdehyde and increased the levels of superoxide dismutase activity in OGD-treated cells. Using western blotting, it was demonstrated that treatment with AA decreased the phosphorylation of p38 and increased the expression of Bcl-2 in

OGD-treated cells. Additionally, the expression of autophagy markers, including beclin-1 and the microtubule-associated proteins 1A/1B light chain 3B II/I ratio, were also decreased in AA treated cells compared with OGD-treated cells. These results demonstrated that AA pretreatment protected cardiomyocytes from ROS-mediated autophagy via a p38 mitogen-activated protein kinase/Bcl-2/beclin-1 signaling pathway in MIRI.

Introduction

Coronary heart disease (CHD) is a significant challenge to human health, and the morbidity and mortality rates are rising rapidly in the United States (1). Currently, treatment for CHD is early reperfusion therapy to open occluded vessels and to prevent ischemia and myocardial infarction (2). However, myocardial ischemia-reperfusion (I/R) injury (MIRI) may result in additional cardiomyocyte dysfunction, which further aggravates myocardial cell damage (3), and constitutes a significant part of the pathology, contributing to heart failure in patients with CHD (4). The mechanisms underlying MIRI are complex and are associated with a variety of pathologies, such as oxidative stress, calcium overload, inflammatory response and energy metabolism disorders (4-6). Among these contributors, a number of studies have demonstrated that oxidative stress induced by a rapid increase in the levels of reactive oxygen species (ROS), which can be observed during reperfusion, is a key initiator of MIRI (6,7).

ROS are metabolites that are produced primarily by mitochondria (8). Under physiological conditions, ROS serve as second messenger signaling molecules, which modulate the intracellular signaling cascade and maintain the normal physiological functions of the cells (9). However, excessive ROS generation during MIRI results in the activation of nuclear factor erythroid 2-related factor 2-associated factors, such as forkhead box O3a and NF- κ B, thereby resulting in an imbalance between oxidation and anti-oxidation in the cells, leading to oxidative stress and ultimately, apoptosis, necrosis or autophagy (10).

Autophagy is an adaptive response of cells to metabolic stresses and environmental alterations. Via lysosome degradation, abnormal proteins, such as misfolded proteins and

Correspondence to: Professor Qiang Wang, Department of Cardiovascular Surgery, Northern Jiangsu People's Hospital, Clinical Medical College, Yangzhou University, 98 West Nantong Road, Yangzhou, Jiangsu 225001, P.R. China
E-mail: wangqiangyz123@163.com

Professor Xiaowei Wang, Department of Thoracic and Cardiovascular Surgery, The First Affiliated Hospital of Nanjing Medical University, 300 Guangzhou Road, Nanjing, Jiangsu 210029, P.R. China
E-mail: wangxiaowein1@163.com

*Contributed equally

Key words: coronary heart disease, myocardial ischemic-reperfusion injury, asiatic acid, autophagy, reactive oxygen species, p38-mitogen-activated protein kinase, B-cell lymphoma-2, beclin-1

damaged organelles, are degraded and recycled to maintain the homeostasis of the intracellular environment (11). Autophagy involves four steps: Induction, formation of autophagosomes, autophagosome and lysosome fusion and degradation of the enclosed substances (11,12). Under normal conditions, the levels of autophagy in cardiomyocytes is low (11). Scherz-Shouval *et al* (13) revealed that increased ROS levels during cellular I/R injury resulted in the upregulation of autophagy, which promoted the degradation of damaged organelles and proteins, thereby reducing the damage caused by oxidative stress to the cells. However, the overactivation of autophagy during reperfusion may destroy important cellular components, resulting in abnormal alterations to the cell structure and the promotion of cell death (11,14). A number of studies have indicated that autophagy serves an important role in MIRI (15,16).

Asiatic acid (AA; $C_{30}H_{48}O_5$; Fig. 1A), which is chemically known as 2,3,23-trihydroxyurs-12-ene-28-oic-acid, is a pentacyclic triterpenoid compound extracted from the traditional Chinese medicinal herb *Centella Asiatica* (17). Previously, numerous studies have demonstrated that AA possesses various pharmacological properties, including hepatoprotective, neuroprotective, antioxidant, anti-inflammatory, anti-hyperglycemic and anticancer properties (18-22). In previous studies, AA was indicated to serve an important role in myocardial protection (23,24). However, to the best of our knowledge, the association of AA with autophagy in MIRI has not been fully investigated. In the present study, *in vivo* and *in vitro* experiments were used to examine the effects of AA on autophagy during MIRI, with the aim of demonstrating the potential pharmacological properties of AA to support its use in the treatment of MIRI.

Materials and methods

Materials. Purified natural extracts of AA (97%) and DMSO were purchased from Merck KGaA. Gibco DMEM and FBS were purchased from Thermo Fisher Scientific, Inc. Cell Counting Kit-8 (CCK-8) was obtained from Dojindo Molecular Technologies, Inc. Total superoxide dismutase (SOD) and lipid peroxidation malondialdehyde (MDA) assay kits were purchased from Beyotime Institute of Biotechnology. All antibodies were purchased from Cell Signaling Technology, Inc. An ECL detection substrate was purchased from Thermo Fisher Scientific, Inc. Unless otherwise indicated, all other chemicals and materials were purchased from Merck KGaA.

Animals and establishment of the mouse MIRI model. A total of 30 Male C57BL/6 mice [purchased from the Experimental Animal Center of Jiangsu Province (Nanjing, China)], weighing 20-25 g and aged 4-6 weeks, were given free access to food and water and were kept under 12:12 h light-dark cycles at room temperature with 40-60% humidity for 1 week for adaptation, after which time all mice were randomized and divided into three groups (n=10 per group) as follows (all treatments were performed once per day for 7 days): Sham operation group, pretreated with PBS for 7 days before the operation; MIRI group, pretreated with PBS for 7 days before the operation; and MIRI + AA group, pretreated with AA (100 mg/kg/day via oral gavage) for 7 days before the operation.

C57BL/6 mice were anesthetized with an intraperitoneal injection of 1% pentobarbital sodium (30 mg/kg) and fixed in the supine position (25). An oral tracheal tube was inserted and connected to an animal ventilator, and the limb-lead electrocardiogram was recorded. The ventilator was assessed to be functioning properly to ensure accurate thoracic surgery could be performed. A lateral incision was performed along the left sternal margin between the third and fourth intercostal muscles to open the skin, intercostal muscles, pleura and to expose the heart. The left anterior descending (LAD) artery was ligated below the junction of the left atrial appendage with a 7-0 prolene thread. ST-segment elevation in the electrocardiogram indicated successful establishment of the model. In the MIRI and MIRI + AA groups, the ligature was removed 30 min after infarction, followed by reperfusion for 24 h. In the sham operation group, the LAD artery was threaded but not ligated, and the remaining operations followed the same procedures as the aforementioned groups.

All aspects of animal care and the experimental protocols to which the animals were subjected were approved by the Animal Care and Use Committee of Nanjing Medical University and performed in accordance with the Guide for the Care and Use of Laboratory Animals, which was published by the United States National Institutes of Health (26). All efforts were made to minimize animal suffering.

Echocardiography. Cardiac function was determined by performing echocardiography on days 0 and 1 after MIRI, using a Vevo® 2100 echocardiograph equipped with a 30-MHz high-resolution phase array transducer (VisualSonics, Inc.). M-mode images were used to obtain the left ventricular parameters [left ventricular end-diastolic diameter (LVEDD), left ventricular end-systolic diameter (LVESD)] that were recorded from two-dimensional images using M-mode interrogation in the short-axis view.

Autophagy measurement. Following cardiac function determination, the animals were sacrificed with intraperitoneal administration of an overdose of pentobarbital sodium (150 mg/kg), death was confirmed by absence of vital signs. The left ventricular cardiac tissue was obtained immediately and fixed with 2.5% glutaraldehyde and 1% citric acid at 4°C overnight. After dehydration with ethanol (50, 70, 80, 90, 95 and 100%) and acetone (100%) in gradient, the tissues were embedded in epoxy resin. Polymerization was performed at 80°C for 24 h. Ultrathin sections (50 µm) were prepared using a ultramicrotome and double-stained with 2% uranium acetate and 10% lead citrate for 1 h at room temperature. Ultrastructural alterations and autophagy in cardiomyocytes were observed under a transmission electron microscope (TEM; cat. no. H-7650; Hitachi, Ltd., magnification, x3,000) at an acceleration voltage of 80 kV. Electron microscopy images were analyzed with ImageJ software v1.46 (National Institutes of Health).

Cell culture and treatment. H9c2 cells were purchased from The Cell Bank of Type Culture Collection of the Chinese Academy of Sciences and cultured as previously described (27). Briefly, H9c2 cells were cultured in high-glucose DMEM supplemented with 10% FBS and 1% penicillin/streptomycin (v/v), in an incubator with 5% CO₂ at 37°C for 48 h.

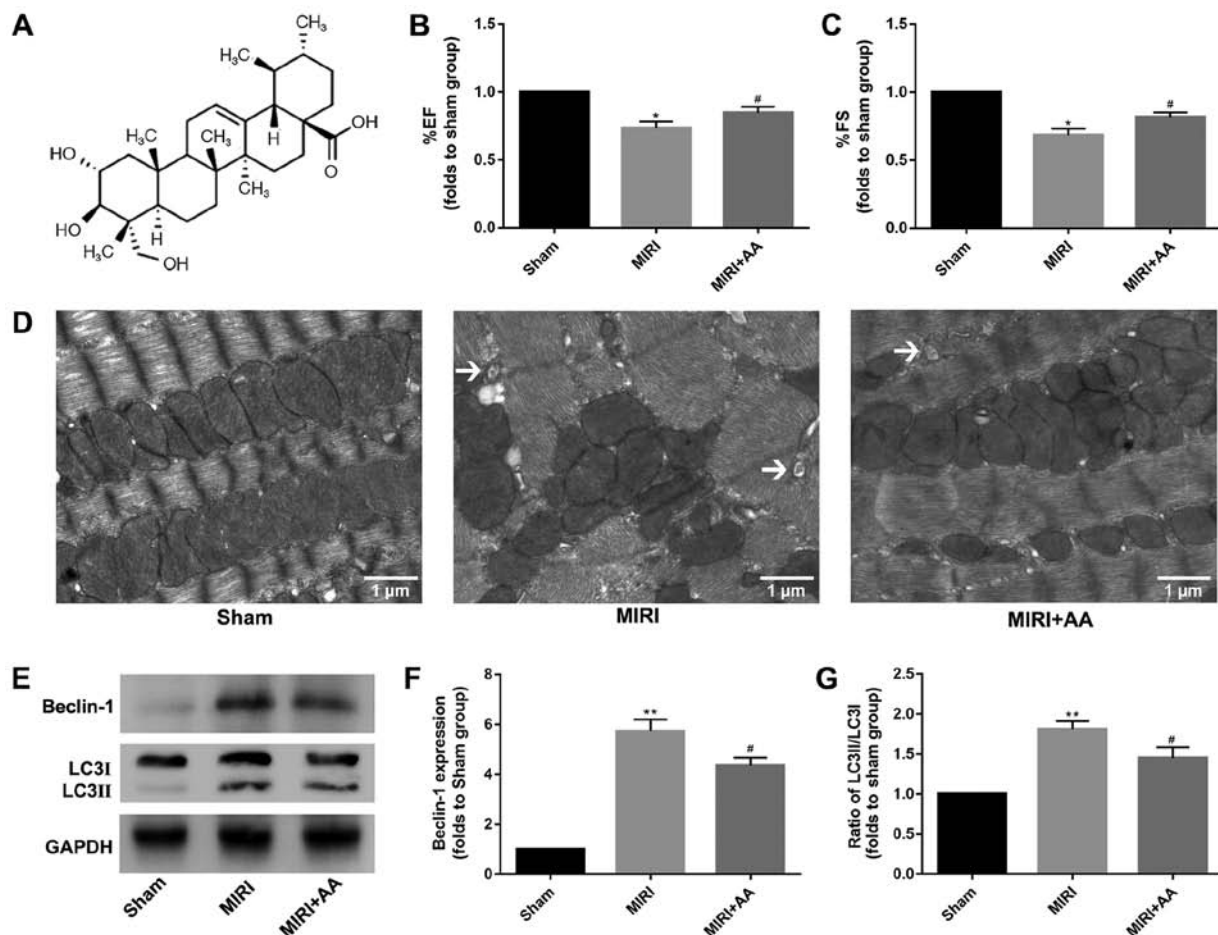


Figure 1. C57BL/6 mice subjected to MIRI in the absence or presence of AA (100 mg/kg/day) pre-treatment for 1 week. (A) Chemical structure of AA. The effect of AA post-MIRI on (B) percent ejection fraction (% EF) and (C) percent fractional shortening (% FS) was detected by echocardiography. * $P < 0.05$ vs. Sham, # $P < 0.05$ vs. MIRI. (D) The effect of AA on mitochondrial damage and autophagy formation induced by MIRI *in vivo* was detected via transmission electron microscopy. The black arrows indicate the autophagosomes. Scale bars, 1 μ m. (E) The effect of AA pre-incubation on the expression levels of the autophagy-associated proteins (F) beclin-1 and (G) LC3 was detected via western blot. The data are presented as the mean \pm standard deviation ($n = 3$). ** $P < 0.01$ vs. Sham; # $P < 0.05$ vs. MIRI. AA, asiatic acid; MIRI, myocardial ischemia-reperfusion injury; LC3, microtubule-associated proteins 1A/1B light chain 3B.

H9c2 cells in logarithmic growth period were plated in a 60 mm culture dish (1×10^6 cells/dish), cultured in an incubator with 5% CO_2 at 37°C for 24 h, and the cell cycle was synchronized using serum-free DMEM for 24 h prior to cell modeling. An oxygen glucose deprivation/reperfusion (OGD) model was established as described previously (28). Cells were placed in an anoxic chamber (Mitsubishi Gas Chemical Company, Inc.) containing AnaeroPack[®] system to create a hypoxic atmosphere. Cells were maintained in hypoxic conditions at 37°C for 6 h, following which pre-equilibrated DMEM containing 10% FBS was added to the cells, and the cells were cultured in a humidified 95% air-5% CO_2 atmosphere at 37°C for an additional 24 h. A total of three groups were used for the *in vitro* experiments: In the control and OGD groups the cells were pretreated with PBS for 24 h prior to OGD modeling at room temperature, and in the OGD + AA group the cells were pretreated with AA (20 μM) for 24 h prior to OGD modeling at room temperature.

Cell viability assay. Cell viability were detected using CCK-8 kit according to the manufacturer's instructions. In brief, the H9c2 cells were initially cultured at a density of 1×10^4 cells/well in 96-well plates at 37°C . The cells were then

pretreated with various concentrations of AA (2.5-100 μM) for 24 h at 37°C . CCK-8 solution (10 μl) was then added to each well and incubated for an additional 2 h at 37°C . The absorbance at 450 nm was measured using a microplate reader (Bio-Rad Laboratories, Inc.). Also, CCK-8 assay was performed after OGD or control treatment. All experiments were performed in triplicate.

Measurement of intracellular ROS levels. ROS generation was determined using the fluorescent probe 2',7'-dichlorofluorescein diacetate (DCFH-DA; Beyotime Institute of Biotechnology). Cell-permeable non-fluorescent DCFH-DA is oxidized to the fluorescent 2',7'-dichlorofluorescein (DCF) in the presence of ROS. H9c2 cells were harvested after the various aforementioned treatments using trypsin. After washing with PBS, 10 μM DCFH-DA was added to the cells for 20 min in the dark at 37°C . The fluorescence intensity was observed under a fluorescence microscope (magnification, $\times 100$; Nikon Corporation) and analyzed using ImageJ software. All experiments were performed in triplicate.

Assessment of oxidative damage. SOD activity and MDA content were measured as the decomposition products of lipid

hydroperoxides. These are often used as indicators of oxidative damage to cells and tissues (25,29,30), and were used in the current *in vitro* study by SOD and MDA assay kits to detect the antioxidant performance of AA according to the manufacturer's protocol. In brief, the H9c2 cells were initially cultured at a density of 1×10^4 cells/well in 96-well plates at 37°C. The cells were sufficiently lysed and centrifuged at 12,000 \times g for 5 min at 4°C after OGD or control treatment. Supernatants were collected to assess SOD activity and MDA content using a microplate reader (Bio-Rad Laboratories, Inc.). All experiments were performed in triplicate.

Western blot analysis. Proteins were extracted from myocardial tissues and H9c2 cells following treatment by ice-cold RIPA lysis buffer (Beyotime Institute of Biotechnology) and the protein concentration was measured using BCA assay (Beyotime Institute of Biotechnology). Protein samples (30 μ g) were loaded onto an 10% SDS gel resolved using SDS-PAGE, transferred to a PVDF membrane, and blocked with 5% skimmed milk for 90 min at room temperature. Subsequently, the membranes were incubated with one of the following antibodies: Anti-microtubule-associated proteins 1A/1B light chain 3B (LC3; cat. no. 3868; Cell Signaling Technology, Inc), anti-B-cell lymphoma-2 (Bcl-2; cat. no. 15071; Cell Signaling Technology, Inc), anti-beclin-1 (cat. no. 3495; Cell Signaling Technology, Inc), anti-phosphorylated-p38 (cat. no. 4511; Cell Signaling Technology, Inc) and anti-p38 (cat. no. 8690; Cell Signaling Technology, Inc) or GAPDH (cat. no. 5174; Cell Signaling Technology, Inc) rabbit polyclonal antibodies, all at 1:1,000 dilution at 4°C overnight. Following incubation with the primary antibodies, the membranes were incubated with the horseradish peroxidase-conjugated goat anti-rabbit secondary antibody (1:2,000; cat. no. 7074; Cell Signaling Technology, Inc) at room temperature for 90 min. Signals were visualized using a chemiluminescence reagent and densitometry analysis was performed using ImageJ software v1.46 (National Institutes of Health). GAPDH was used as the loading control. All experiments were performed in triplicate.

Statistical analysis. Data are expressed as the mean \pm standard deviation. Differences between groups were compared using one-way ANOVA. Statistical analysis was performed using GraphPad Prism v7 (GraphPad Software, Inc.) and PASW Statistics v18.0 (SPSS, Inc.). Comparisons between two groups were performed using unpaired two-tailed Student's t-test. Comparisons between more than two groups were performed using one-way ANOVA and Tukey's post hoc tests. $P < 0.05$ was considered to indicate a statistically significant difference. All experiments were performed in triplicate.

Results

AA improves cardiac function in mice with MIRI. Cardiac function was similar among mice in all groups prior to MIRI treatment (data not shown). However, the echocardiography evaluation revealed significant decreases in percent ejection fraction and percent fractional shortening in MIRI mice at 24 h post-reperfusion compared with sham mice, and pretreatment with AA partially rescued MIRI-induced cardiac impairment (Fig. 1B and C).

MIRI initiates an autophagic response in murine hearts. TEM is considered as the gold standard for identifying double-membrane vacuole structures (31-33). Autophagy activation during MIRI was first measured via ultrastructural analysis using TEM. As demonstrated in Fig. 1D, the degree of mitochondrial destruction and the number of autophagosomes in myocardial cells that underwent MIRI were higher compared with the sham group. AA pretreatment was indicated to attenuate the mitochondrial damage and autophagosome formation in injured cardiomyocytes. The autophagy-associated proteins beclin-1 and LC3 were used to evaluate the levels of intracellular autophagy (34,35), and their expression was examined via western blotting. The expression levels of beclin-1 and the ratio of LC3 II/I were increased following MIRI compared with the sham group, whereas AA pretreatment lowered these levels (Fig. 1E-G). Taken together, these results suggest that autophagy is associated with MIRI, and that AA pretreatment partially reduces autophagy following MIRI.

MIRI decreases and AA restores cell viability. The chemical structure of AA is presented in Fig. 1A. To determine the optimal AA concentration for treatment of cardiomyocytes *in vitro*, an AA dose-response curve was plotted, and it was demonstrated that the viability of H9c2 cells was impaired when treated with AA concentrations $>20 \mu$ M. Therefore, 20 μ M AA was used for all subsequent *in vitro* experiments (Fig. 2A). Based on the CCK-8 assay (Fig. 2B), H9c2 viability was reduced by OGD treatment compared with the control cells, whereas AA pre-treatment protected myocardial cells from OGD treatment.

AA attenuates the increased production of intracellular ROS induced by MIRI. DCF intensity was used to measure the intracellular ROS production. The effects of OGD treatment on ROS production in cardiomyocytes are presented in Fig. 2C and D. H9c2 cells treated with OGD exhibited a prominent increase in fluorescence intensity compared with the control group, and AA pretreatment reduced the production of ROS, which was mediated by OGD. The intracellular MDA levels and SOD activity were additionally measured to support the antioxidant function of AA. As demonstrated in Fig. 2E and F, increased levels of MDA and reduced SOD activity were observed in OGD-treated cells compared with the control group, suggesting the presence of an increased oxidative stress and the failure of the antioxidant responses to alleviate stress resulting from OGD. However, AA pretreatment decreased the MDA levels and increased SOD activity, compared with the OGD group. Taken together, these results suggest that the protective effects of AA against the OGD-induced cardiomyocyte injury were associated with the alleviation of oxidative stress, which was mediated by ROS.

OGD induces autophagy in vitro. The expression of autophagy-associated proteins was measured in OGD-treated cardiomyocytes. Compared with cardiomyocytes in the control group, OGD induced cardiomyocyte autophagy, which was reflected by the increased beclin-1 expression and LC3 II/I ratio, as indicated via western blotting. AA pretreatment partially suppressed the effects of OGD on autophagy in cardiomyocytes *in vitro* (Fig. 3A-C).

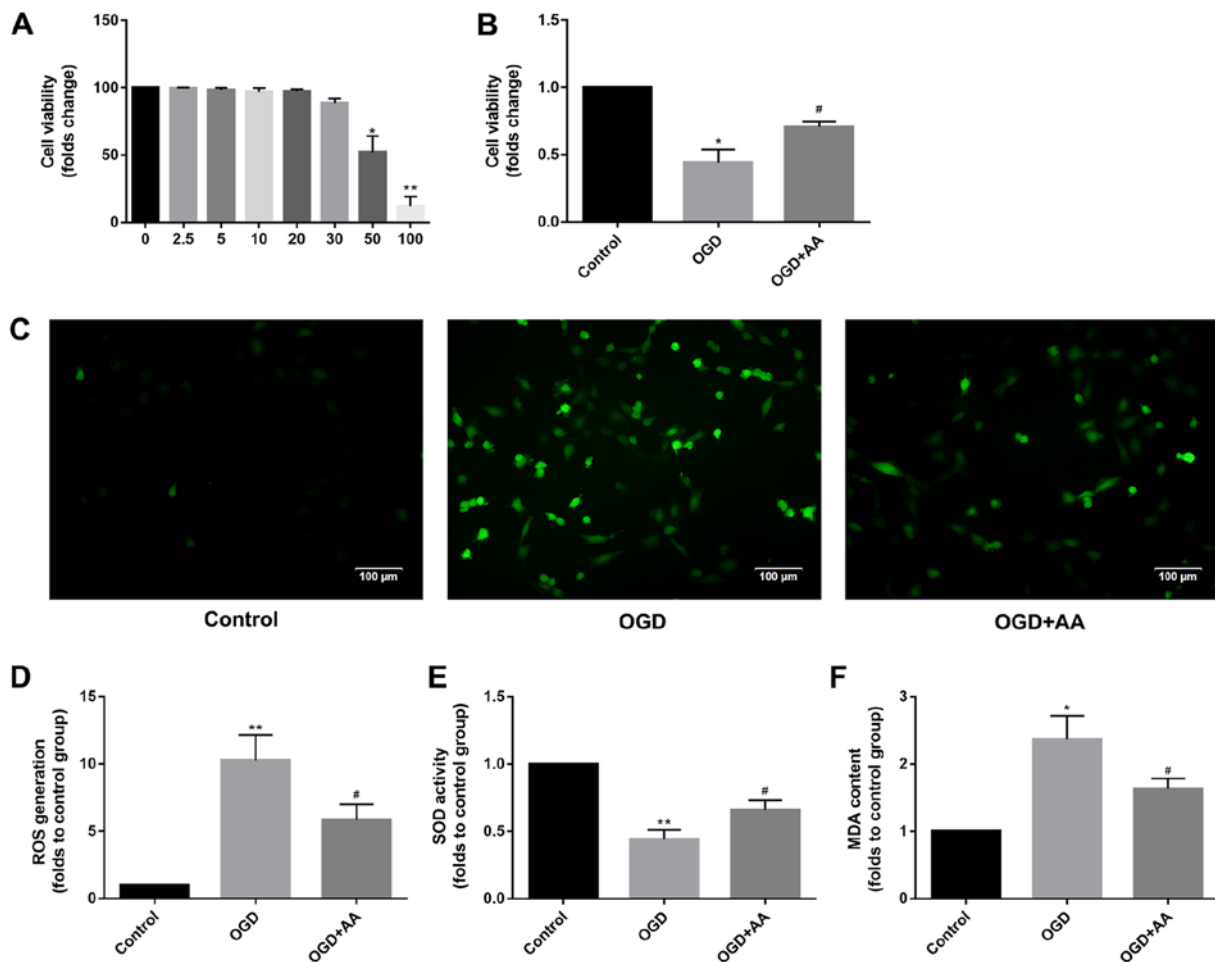


Figure 2. Protective effects of AA on OGD-induced oxidative stress in H9c2 cells. (A) The cytotoxicity of AA on H9c2 cells was assessed via the CCK-8 assay. 20 μ M was chosen as the dose of AA for the following study. The data are presented as the mean \pm SD. * P <0.05 and ** P <0.01 vs. 0 mM. (B) The viability of H9c2 cells after OGD or control treatment was measured via the CCK-8 assay. The data are presented as the mean \pm SD. * P <0.05 vs. Control; # P <0.05 vs. OGD. (C) ROS mediate the OGD-induced autophagy in H9c2 cells. H9c2 cells were subjected to OGD in the absence or presence of the AA. The cells were incubated with 2',7'-dichlorofluorescein diacetate and fluorescence was measured using a fluorescence microscope. Representative images (magnification, \times 100) are presented to indicate ROS levels. Scale bars, 100 μ m. The data are presented as the mean \pm SD. (D) ImageJ software was used to perform a quantitative analysis of intracellular ROS production. ** P <0.01 vs. Control; # P <0.05 vs. OGD. The (E) SOD activity and (F) intracellular MDA production was measured in H9c2 cells after OGD or control treatment. The data are presented as the mean \pm SD. * P <0.05 and ** P <0.01 vs. Control; # P <0.05 vs. OGD. AA, asiatic acid; CCK-8, cell counting kit-8; OGD, glucose deprivation/reperfusion; ROS, reactive oxygen species; SD, standard deviation; SOD, superoxide dismutase; MDA, malondialdehyde.

OGD regulates p38/Bcl-2 signaling, which is attenuated by AA. The Bcl-2/beclin-1 complex is a key regulator of autophagy (36). As indicated via western blot analysis, MIRI reduced the protein expression levels of Bcl-2 (Fig. 3A and D). This may underlie the increased expression of beclin-1 in MIRI. A variety of protein kinases, including mitogen-activated protein kinase (MAPK) family members, have been reported to induce Bcl-2 phosphorylation in other cell systems (37,38). In the present study, p38-MAPK was selected for subsequent analysis, and phosphorylation of p38 was increased following OGD stimulation. AA pretreatment reduced the degree of p38 phosphorylation (Fig. 4) and increased Bcl-2 expression (Fig. 3A and D), compared with the OGD group.

Discussion

Thanks to the continuous advances in cell biology, it has been demonstrated that in addition to necrosis and apoptosis, MIRI also results in autophagy in cardiomyocytes (15,39,40). In 1976,

Sybers *et al* (41) demonstrated that autophagosomes containing damaged organelles were detected following reoxygenation and glucose administration in hypoglycemic cells *in vitro*. This was the first report of autophagy in MIRI. Subsequently, Decker *et al* (42) reported an important increase in autophagy in rabbit hearts after 40 min of I/R. Matsui *et al* (14) demonstrated that the expression of LC3 was increased in a mouse model of MIRI, reflecting the enhancement of myocardial autophagy. Several factors have been reported to be associated with MIRI, including oxidative stress, and ROS has been indicated to induce autophagy (43); however, how ROS-mediated oxidative stress initiates the autophagic response remains unclear.

Beclin-1 is an autophagy-associated protein with homology to autophagy-related protein 6, which is a key factor regulating autophagy (44). Beclin-1 initiates autophagy and promotes the formation of autophagic lysosomes (45). Structurally, beclin-1 has been indicated to contain three identifiable domains: A short Bcl-2-homology (BH) 3 motif,

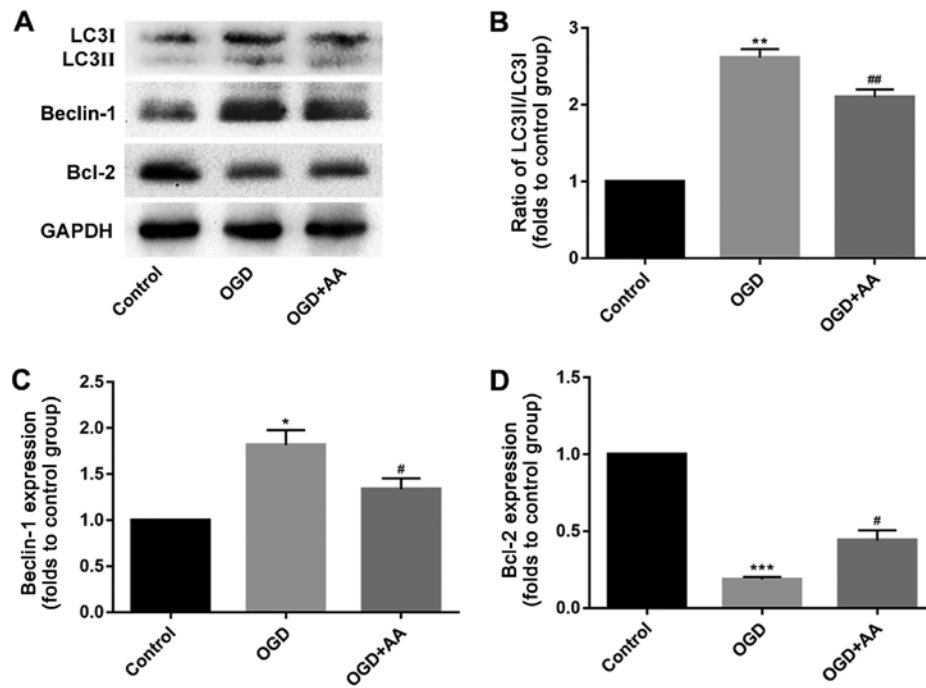


Figure 3. AA attenuates autophagy in H9c2 cells after OGD treatment. The expression of autophagy-associated proteins was measured using a western-blot assay. (A) The protein levels of beclin-1, LC3 and Bcl-2 were detected via western blotting. The expression levels of (B) LC3, (C) beclin-1 and (D) Bcl-2 were quantified using the ImageJ software. The data are presented as the mean \pm standard deviation. * P <0.05, ** P <0.01 and *** P <0.001 vs. Control; # P <0.05, ## P <0.01 vs. OGD. AA, asiatic acid; OGD, glucose deprivation/reperfusion; LC3, microtubule-associated proteins 1A/1B light chain 3B; Bcl-2, B-cell lymphoma-2.

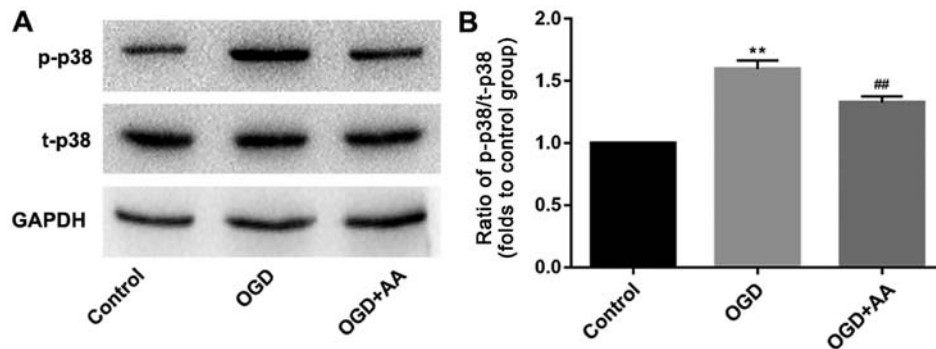


Figure 4. ROS-dependent activation of p38-MAPK is associated with the induction of autophagy in myocardial ischemia-reperfusion injury. H9c2 cells were pretreated with AA (20 μ M) followed by OGD treatment. (A) Western blot analysis was used to detect the protein expression of p-p38 and t-p38 MAPK. (B) ImageJ software was used to perform a quantitative analysis of p-p38/t-p38 MAPK. The data are presented as the mean \pm standard deviation. ** P <0.01 vs. Control; ## P <0.01 vs. OGD. AA, asiatic acid; OGD, glucose deprivation/reperfusion; p, phospho; t, total; MAPK, mitogen-activated protein kinase.

a central coiled-coil domain and a C-terminal half, which encompasses the evolutionarily conserved domain (46). Beclin-1 has been revealed to form protein complexes with autophagy regulatory proteins, thereby regulating autophagy levels (44,45,47). Matsui *et al* (14) demonstrated that autophagy during MIRI was beclin-1-dependent, and primarily manifested following increased beclin-1 expression during myocardial reperfusion, whereas knockout of the beclin-1 gene inhibited the formation of autophagosomes during reperfusion. This result was also confirmed by Valentim *et al* (39) who demonstrated that when the expression of beclin-1 in cardiomyocytes was decreased, autophagy was also reduced. Bcl-2 is an endogenous inhibitor of beclin-1 (48). Previous studies have indicated the existence of a direct association between the balance of Bcl-2 and

beclin-1 protein expression, which has been demonstrated to affect autophagy levels (37,49). Physiologically, beclin-1 binds to the BH3 domain of Bcl-2 to form a complex, and this Bcl-2/beclin-1 complex ensures that autophagy levels remain within a homeostatic range (49). However, when beclin-1 function is not regulated by Bcl-2 or potentially other Bcl-2 family members, including Bcl-XL, this may result in excessive levels of autophagy (49). During MIRI, the excessive accumulation of ROS results in increased phosphorylation of Bcl-2, disrupting the balance between Bcl-2 and beclin-1. The subsequent dissociation of the Bcl-2/beclin-1 complex causes the release of large quantities of beclin-1, which results in excessive autophagy and, possibly, autophagy-dependent cell death (25). Therefore, the balance between Bcl-2 and beclin-1 appears to underlie the activation of autophagy.

Multiple signaling pathways are associated with ROS-mediated autophagy, including the MAPK signaling pathways (50). MAPK is an important transmembrane signaling pathway that is composed of three major MAPK cascades, p38, ERK1/2 and JNK, which serve a critical role during cell proliferation, differentiation and apoptosis (51-53). Oxidative stress has been indicated to activate MAPK subfamilies in cardiomyocytes (54). The dynamic balance between the effects of MAPKs are important for determining cell fate (27,43). p38-MAPK appears to be more sensitive to oxidative stress compared with other MAPKs, such as ERK1/2 and JNK (37). Additionally, several studies have demonstrated that ROS-dependent p38 activation regulates Bcl-2 via phosphorylation, which results in autophagy or apoptosis (27,55).

AA exerts beneficial effects against I/R injury. For example, Xu *et al* (56) reported that AA was effective in mitigating hepatic I/R injury and inducing the attenuation of Kupffer cell activation via a peroxisome proliferator-activated receptor gamma/NACHT, LRR and PYD domains-containing protein 3 inflammasome signaling pathway. Lu *et al* (57) demonstrated that AA attenuated the I/R-induced liver damage via reducing the oxidative stress and restoring the mitochondrial function. In MIRI, Huang *et al* (58) demonstrated that AA induced activation of the Akt/glycogen synthase kinase-3 β /hypoxia-inducible factor 1- α pathway, and may contribute to the suppression of ROS accumulation and mitochondrial dysfunction in MIRI injury. However, the results of Huang *et al* (58) were limited to *in vitro* experiments and did not illustrate the roles of AA *in vivo*. The results of the present study demonstrated that pretreatment with AA was protective against MIRI-induced cell damage thanks to its antioxidant and autophagy-suppressing properties. *In vivo* experiments revealed that AA pretreatment improved cardiac function and attenuated autophagy in injured cardiomyocytes, which was evidenced by the reduced mitochondrial damage, the decreased autophagosome formation and the reduced expression of autophagy-associated proteins. Additionally, the *in vitro* experiments demonstrated that AA reduced ROS production, which was induced by OGD, a cellular model of MIRI, decreased the phosphorylation of p38 and increased the expression of Bcl-2 to stabilize the Bcl-2/beclin-1 complex, thereby suppressing the dissociation of beclin-1 and the occurrence of autophagy.

In conclusion, the present study suggested that AA protected cardiomyocytes from ROS-mediated autophagy via a p38-MAPK/Bcl-2 signaling pathway in MIRI. This may be a novel mechanism underlying the protective effects of AA in cardiomyopathy. However, additional studies are required to determine whether AA may be used as a potential treatment in the clinical setting.

Acknowledgements

Not applicable.

Funding

The present study was funded by a research project of Northern Jiangsu People's Hospital (grant no. yzucms201621),

the National Natural Science Foundation of China (grant nos. 81573234 and 81773445) and the '333 Project' Of Jiangsu Province (grant no. LGY2016006).

Availability of data and materials

The datasets used and/or analyzed during the current study are available from the corresponding author on reasonable request.

Authors' contributions

CY, LS, JX and JY performed the experiments, analyzed the data and prepared the manuscript. QW and XW wrote and revised the manuscript, and designed the experiments. All authors read and approved the final manuscript.

Ethics approval and consent to participate

All aspects of animal care and the experimental protocols to which the animals were subjected were approved by the Animal Care and Use Committee of Nanjing Medical University and conducted in accordance with the Guide for the Care and Use of Laboratory Animals, published by the United States National Institutes of Health (23). All efforts were made to minimize animal suffering.

Patient consent for publication

Not applicable.

Competing interests

The authors declare that they have no competing interests.

References

1. Rai V, Sharma PK, Agrawal S and Agrawal DK: Relevance of mouse models of cardiac fibrosis and hypertrophy in cardiac research. *Mol Cell Biochem* 424: 123-145, 2017.
2. Sharma V, Bell RM and Yellon DM: Targeting reperfusion injury in acute myocardial infarction: A review of reperfusion injury pharmacotherapy. *Expert Opin Pharmacother* 13: 1153-1175, 2012.
3. Hearse DJ and Bolli R: Reperfusion induced injury: Manifestations, mechanisms, and clinical relevance. *Cardiovasc Res* 26: 101-108, 1992.
4. Eltzschig HK and Eckle T: Ischemia and reperfusion-from mechanism to translation. *Nat Med* 17: 1391-1401, 2011.
5. Murphy E and Steenbergen CJ: Mechanisms Underlying acute protection from cardiac ischemia-reperfusion injury. *Physiol Rev* 88: 581-609, 2008.
6. Zhao Q, Liu Z, Huang B, Yuan Y, Liu X, Zhang H, Qiu F, Zhang Y, Li Y, Miao H, *et al*: PEDF improves cardiac function in rats subjected to myocardial ischemia/reperfusion injury by inhibiting ROS generation via PEDF-R. *Int J Mol Med* 41: 3243-3252, 2018.
7. Ferrari RS and Andrade CF: Oxidative stress and lung ischemia-reperfusion injury. *Oxid Med Cell Longev* 2015: 590987, 2015.
8. Zhou T, Chuang CC and Zuo L: Molecular characterization of reactive oxygen species in myocardial ischemia-reperfusion injury. *Biomed Res Int* 2015: 864946, 2015.
9. Toda C and Diano S: Mitochondrial UCP2 in the central regulation of metabolism. *Best Pract Res Clin Endocrinol Metab* 28: 757-764, 2014.
10. Saeed-Zidane M, Linden L, Salilew-Wondim D, Held E, Neuhooff C, Tholen E, Hoelker M, Schellander K and Tesfaye D: Cellular and exosome mediated molecular defense mechanism in bovine granulosa cells exposed to oxidative stress. *PLoS One* 12: e0187569, 2017.

11. Przyklenk K, Dong Y, Undyala VV and Whittaker P: Autophagy as a therapeutic target for ischaemia/reperfusion injury? Concepts, controversies, and challenges. *Cardiovasc Res* 94: 197-205, 2012.
12. Klionsky DJ and Emr SD: Autophagy as a regulated pathway of cellular degradation. *Science* 290: 1717-1721, 2000.
13. Scherz-Shouval R and Elazar Z: Regulation of autophagy by ROS: Physiology and pathology. *Trends Biochem Sci* 36: 30-38, 2011.
14. Matsui Y, Takagi H, Qu X, Abdellatif M, Sakoda H, Asano T, Levine B and Sadoshima J: Distinct roles of autophagy in the heart during ischemia and reperfusion: Roles of AMP-activated Protein Kinase and Beclin 1 in Mediating Autophagy. *Circ Res* 100: 914-922, 2007.
15. Dong Y, Undyala VV, Gottlieb RA, Mentzer RM Jr and Przyklenk K: Autophagy: Definition, molecular machinery, and potential role in myocardial ischemia-reperfusion injury. *J Cardiovasc Pharmacol Ther* 15: 220-230, 2010.
16. Abounit K: The process of autophagy in an in vitro model of myocardial ischemia-reperfusion injury. *Dissertations & Theses-Gradworks* 2011.
17. Lv J, Sharma A, Zhang T, Wu Y and Ding X: Pharmacological review on asiatic acid and its derivatives: A potential compound. *SLAS Technol* 23: 111-127, 2018.
18. Duggina P, Kalla CM, Varikasuvu SR, Bukke S and Tartte V: Protective effect of centella triterpene saponins against cyclophosphamide-induced immune and hepatic system dysfunction in rats: Its possible mechanisms of action. *J Physiol Biochem* 71: 435-454, 2015.
19. Ternchoocheep K, Surangkul D and Ysothonsreekul S: The recovery and protective effects of asiatic acid on differentiated human neuroblastoma SH-SY5Y cells cytotoxic-induced by cholesterol. *Asian Pacific J Tropical Biomedicine* 7: 416-420, 2017.
20. Huang SS, Chiu CS, Chen HJ, Hou WC, Sheu MJ, Lin YC, Shie PH and Huang GJ: Antinociceptive activities and the mechanisms of anti-inflammation of asiatic acid in mice. *Evid Based Complement Alternat Med* 2011: 895857, 2011.
21. Chun F: Asiatic acid protects hearts and relative mitochondria of streptozotocin-induced diabetic rats. *J Jiangsu University* 2010.
22. Goncalves B, Salvador JAR, Marin S and Cascante M: Synthesis and biological evaluation of novel asiatic acid derivatives with anticancer activity. *RSC Adv* 6: 3967-3985, 2016.
23. Si L, Xu J, Yi C, Xu X, Ma C, Yang J, Wang F, Zhang Y and Wang X: Asiatic acid attenuates the progression of left ventricular hypertrophy and heart failure induced by pressure overload by inhibiting myocardial remodeling in mice. *J Cardiovasc Pharmacol* 66: 558-568, 2015.
24. Xu X, Si L, Xu J, Yi C, Wang F, Gu W, Zhang Y and Wang X: Asiatic acid inhibits cardiac hypertrophy by blocking interleukin-1 β -activated nuclear factor- κ B signaling in vitro and in vivo. *J Thorac Dis* 7: 1787-1797, 2015.
25. Tang Z, Yang L and Zhang X: Vitexin mitigates myocardial ischemia reperfusion-induced damage by inhibiting excessive autophagy to suppress apoptosis via the PI3K/Akt/mTOR signaling cascade. *RSC Adv* 7: 56406-56416, 2017.
26. Clark JD, Gebhart GF, Gonder JC, Keeling ME and Kohn DF: Special report: The 1996 Guide for the care and use of laboratory animals. *ILAR J* 38: 41-48, 1997.
27. Liu J, Chang F, Li F, Fu H, Wang J, Zhang S, Zhao J and Yin D: Palmitate promotes autophagy and apoptosis through ROS-dependent JNK and p38 MAPK. *Biochem Biophys Res Commun* 463: 262-267, 2015.
28. Kamiya T, Kown AH, Kanemaki T, Matsui Y, Uetsuji S, Okumura T and Kamiyama Y: A simplified model of hypoxic injury in primary cultured rat hepatocytes. *In Vitro Cell Dev Biol Anim* 34: 131-137, 1998.
29. Jomova K and Valko M: Advances in metal-induced oxidative stress and human disease. *Toxicology* 283: 65-87, 2011.
30. Ray G, Batra S, Shukla NK, Deo S, Raina V, Ashok S and Husain SA: Lipid peroxidation, free radical production and antioxidant status in breast cancer. *Breast Cancer Res Treat* 59: 163-170, 2000.
31. Eskelinen E, Reggiori F, Baba M, Kovacs AL and Seglen PO: Seeing is believing: The impact of electron microscopy on autophagy research. *Autophagy* 7: 935-956, 2011.
32. Martinet W, Timmermans J and De Meyer GR: Methods to assess autophagy in situ-transmission electron microscopy versus immunohistochemistry. *Methods Enzymol* 543: 89-114, 2014.
33. Nadal M and Gold SE: Assessment of autophagosome formation by transmission electron microscopy. *Methods Mol Biol* 835: 481-489, 2012.
34. Pattingre S, Espert L, Biard-Piechaczyk M and Codogno P: Regulation of macroautophagy by mTOR and Beclin 1 complexes. *Biochimie* 90: 313-323, 2008.
35. Mizushima N and Yoshimori T: How to interpret LC3 immunoblotting. *Autophagy* 3: 542-545, 2007.
36. Marquez RT and Xu L: Bcl-2:Beclin 1 complex: Multiple, mechanisms regulating autophagy/apoptosis toggle switch. *Am J Cancer Res* 2: 214-221, 2012.
37. Markou T, Dowling AA, Kelly T and Lazou A: Regulation of Bcl-2 phosphorylation in response to oxidative stress in cardiac myocytes. *Free Radic Res* 43: 809-816, 2009.
38. De Chiara G, Marcocci ME, Torcia M, Lucibello M, Rosini P, Bonini P, Higashimoto Y, Damonte G, Armirotti A, Amodei S, *et al*: Bcl-2 Phosphorylation by p38 MAPK: Identification of target sites and biologic consequences. *J Biol Chem* 281: 21353-21361, 2006.
39. Valentim L, Laurence KM, Townsend PA, Carroll CJ, Soond S, Scarabelli TM, Knight RA, Latchman DS and Stephanou A: Urocortin inhibits Beclin1-mediated autophagic cell death in cardiac myocytes exposed to ischaemia/reperfusion injury. *J Mol Cell Cardiol* 40: 846-852, 2006.
40. Aghaei M, Motalebnezhad M, Ghorghanlu S, Jabbari A, Enayati A, Rajaei M, Pourabouk M, Moradi A, Alizadeh AM and Khori V: Targeting autophagy in cardiac ischemia/reperfusion injury: A novel therapeutic strategy. *J Cell Physiol* 234: 16768-16778, 2019.
41. Sybers HD, Ingwall J and Deluca M: Autophagy in cardiac myocytes. *Recent Adv Stud Cardiac Struct Metab* 12: 453-463, 1976.
42. Decker RS and Wildenthal K: Lysosomal alterations in hypoxic and reoxygenated hearts. I. Ultrastructural and cytochemical changes. *Am J Pathol* 98: 425-444, 1980.
43. Guo C, Yang M, Jing L, Wang J, Yu Y, Li Y, Duan J, Zhou X, Li Y and Sun Z: Amorphous silica nanoparticles trigger vascular endothelial cell injury through apoptosis and autophagy via reactive oxygen species-mediated MAPK/Bcl-2 and PI3K/Akt/mTOR signaling. *Int J Nanomedicine* 11: 5257-5276, 2016.
44. Cao Y and Klionsky DJ: Physiological functions of Atg6/Beclin 1: A unique autophagy-related protein. *Cell Res* 17: 839-849, 2007.
45. Bellot G, Garcia-Medina R, Gounon P, Chiche J, Roux D, Pouyssegur J and Mazure NM: Hypoxia-Induced autophagy is mediated through hypoxia-inducible factor induction of BNIP3 and BNIP3L via Their BH3 Domains. *Mol Cell Biol* 29: 2570-2581, 2009.
46. Fu LL, Cheng Y and Liu B: Beclin-1: Autophagic regulator and therapeutic target in cancer. *Int J Biochem Cell Biol* 45: 921-924, 2013.
47. Kang R, Zeh HJ, Lotze MT and Tang D: The Beclin 1 network regulates autophagy and apoptosis. *Cell Death Differ* 18: 571-580, 2011.
48. Matsunaga K, Saitoh T, Tabata K, Omori H, Satoh T, Kurotori N, Maejima I, Shirahama-Noda K, Ichimura T, Isobe T, *et al*: Two Beclin 1-binding proteins, Atg14L and Rubicon, reciprocally regulate autophagy at different stages. *Nat Cell Biol* 11: 385-396, 2009.
49. Pattingre S, Tassa A, Qu X, Garuti R, Liang XH, Mizushima N, Packer M, Schneider MD and Levine B: Bcl-2 antiapoptotic proteins inhibit Beclin 1-dependent autophagy. *Cell* 122: 927-939, 2005.
50. Kulisz A, Chen N, Chandel NS, Shao Z and Schumacker PT: Mitochondrial ROS initiate phosphorylation of p38 MAP kinase during hypoxia in cardiomyocytes. *Am J Physiol Lung Cell Mol Physiol* 282: 1324-1329, 2002.
51. Wada T and Penninger JM: Mitogen-activated protein kinases in apoptosis regulation. *Oncogene* 23: 2838-2849, 2004.
52. Chang L and Karin M: Mammalian MAP kinase signalling cascades. *Nature* 410: 37-40, 2001.
53. Kong D, Zheng T, Zhang M, Wang D, Du S, Li X, Fang J and Cao X: Static mechanical stress induces apoptosis in rat endplate chondrocytes through MAPK and mitochondria-dependent caspase activation signaling pathways. *PLoS One* 8: e69403, 2013.
54. Becatti M, Taddei N, Cecchi C, Nassi N, Nassi PA and Fiorillo C: SIRT1 modulates MAPK pathways in ischemic-reperfused cardiomyocytes. *Cell Mol Life Sci* 69: 2245-2260, 2012.

55. Ranawat P and Bansal MP: Apoptosis induced by modulation in selenium status involves p38 MAPK and ROS: Implications in spermatogenesis. *Mol Cell Biochem* 330: 83-95, 2009.
56. Xu Y, Yao J, Zou C, Zhang H, Zhang S, Liu J, Ma G, Jiang P and Zhang W: Asiatic acid protects against hepatic ischemia/reperfusion injury by inactivation of Kupffer cells via PPAR γ /NLRP3 inflammasome signaling pathway. *Oncotarget* 8: 86339-86355, 2017.
57. Lu Y, Kan H, Wang Y, Wang D, Wang X, Gao J and Zhu L: Asiatic acid ameliorates hepatic ischemia/reperfusion injury in rats via mitochondria-targeted protective mechanism. *Toxicol Appl Pharmacol* 338: 214-223, 2018.
58. Huang X, Zuo L, Lv Y, Chen C, Yang Y, Xin H, Li Y and Qian Y: Asiatic acid attenuates myocardial ischemia/reperfusion injury via Akt/GSK-3 β /HIF-1 α signaling in rat H9c2 cardiomyocytes. *Molecules* 21: 1248, 2016.



This work is licensed under a Creative Commons Attribution-NonCommercial-NoDerivatives 4.0 International (CC BY-NC-ND 4.0) License.